FTIR spectroscopic study of low temperature NO adsorption and NO+O-2 coadsorption on H-ZSM-5

6 AUTHORS, INCLUDING:

A. Penkova
Universidad de Sevilla
20 PUBLICATIONS   **275** CITATIONS

SEE PROFILE

Konstantin Hadjiivanov
Bulgarian Academy of Sciences
195 PUBLICATIONS   **6,001** CITATIONS

SEE PROFILE

Mihail Yordanov Mihaylov
Bulgarian Academy of Sciences
58 PUBLICATIONS   **993** CITATIONS

SEE PROFILE

Marco Daturi
Université de Caen Normandie
250 PUBLICATIONS   **7,086** CITATIONS

SEE PROFILE

FTIR Spectroscopic Study of Low Temperature NO Adsorption and NO + O₂ Coadsorption on H−ZSM-5

A. Penkova,[†] K. Hadjiivanov,*,[†] M. Mihaylov,[†] M. Daturi,[‡] J. Saussey,[‡] and
J.-C. Lavalley[‡]

*Institute of General and Inorganic Chemistry, Bulgarian Academy of Sciences,
Sofia 1113, Bulgaria, and Laboratoire Catalyse et Spectrochimie, CNRS-ISMRA,
Université de Caen, 6, bd Maréchal Juin, 14050 Caen Cedex, France*

Adsorption of NO and coadsorption of NO and O_2 on H−ZSM-5 have been studied at low and room temperature by means of FTIR spectroscopy. For better interpretation of the spectra, experiments involving isotopic labeled molecules have been performed. Low temperature adsorption of NO on H−ZSM-5 results initially in formation of NO which is H-bonded to the zeolite acidic hydroxyls. A second NO molecule is inserted into the OH−NO species at higher coverages, thus forming $OH(NO)_2$ complexes. Different kinds of NO dimers are also formed. Negligible amounts of oxygenated compounds have been detected. In the presence of oxygen, the (di)nitrosyl species are oxidized very fast even at 100 K to N_2O_3, NO^+, NO_2, and N_2O_4. Different kinds of adsorbed N_2O_3 species have been evidenced. With increasing temperature, NO^+ migrates and occupies cationic positions. The latter species interacts with NO at low temperature to give an $[ONNO]^+$ complex. This reaction is used to prove that the different bands in the $2206-2180$ cm^{-1} region are also due to NO^+ species.

1. Introduction

Detailed knowledge of the nature of nitrogen-oxo species formed during adsorption of NO under aerobic and anaerobic conditions is very important for the understanding of the mechanism of different NO_x conversion reactions. In particular, big attention has been recently paid to different metal-exchanged ZSM-5 samples, since they are reported to be among the most promising catalysts for direct NO decomposition and selective catalytic reduction with hydrocarbons.[1−20] It should be noted that, in many cases, residual protons are present on the samples. Moreover, in some cases, the protonic acidity is decisive for the good catalytic performance.[11] Therefore, detailed knowledge of the nature of species formed after NO adsorption under aerobic and anaerobic conditions on H−ZSM-5 is of a definite interest.

There are some detailed investigations on this problem,[21−24] but all of them have been performed at ambient temperature. The main achievements can be summarized as follows:

(1) NO is practically not adsorbed on H−ZSM-5 at ambient temperature.[21]

(2) Coadsorption of NO and O_2 leads to the formation of NO^+ which is formed according to the following reactions:

$$2NO + O_2 \rightarrow 2NO_2 \tag{1}$$

$$NO + NO_2 \rightarrow N_2O_3 \tag{2}$$

$$2O-H^+ + N_2O_3 \rightarrow H_2O + 2O-NO^+ \tag{3}$$
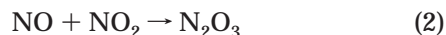
The NO^+ produced is characterized by a band at 2133 cm^{-1}.[21] This band has almost the same position with different Me-exchanged ZSM-5 samples[12−19] and is usually

* Corresponding author. Fax: +003592 8705024. Phone: +003592 9793598. E-mail: kih@svr.igic.bas.bg.
† Bulgarian Academy of Sciences.
‡ Université de Caen.

(1) Iwamoto, M.; Furukawa, H.; Kagawa, S. In *New Developments in Zeolite Science and Technology*, Proceedings from the 7th International Zeolite Conference, Tokyo, August 17−22, 1986; Murakami, Y., Lijima, A., Ward, J. W., Eds.; Kadansha: Tokyo (Elsevier: Amsterdam, The Netherlands), 1986; p 943.
(2) Li, Y.; Slager, T. L.; Armor, J. N. *J. Catal.* **1994**, *150*, 388.
(3) Hadjiivanov, K.; Klissurski, D.; Ramis, G.; Busca, G. *Appl. Catal., B* **1996**, *7*, 251.
(4) Lobree, L. J.; Hwang, I. G.; Reimer, J. A.; Bell, A. T. *J. Catal.* **1999**, *186*, 242.
(5) Chen, H. Y.; Voskoboinikov, T.; Sachtler, W. M. H. *Catal. Today* **1999**, *54*, 483.
(6) Hadjiivanov, K.; Knözinger, H.; Tsyntsarski, B.; Dimitrov, L. *Catal. Lett.* **1999**, *62*, 35.
(7) Mihaylov, M.; Hadjiivanov, K. *Langmuir* **2002**, *18*, 4376.
(8) Hadjiivanov, K.; Ivanova, E.; Daturi, M.; Saussey, J.; Lavalley, J.-C. *Chem. Phys. Lett.* **2003**, *370*, 712.
(9) Mul, G.; Perez-Ramirez, J.; Kapteijn, F.; Moulijn, J. A. *Catal. Lett.* **2001**, *77*, 7.
(10) Sobczak, I.; Decyk, P.; Ziolek, M.; Daturi, M.; Lavalley, J.-C.; Kevan, L.; Prakash, A. M. *J. Catal.* **2002**, *207*, 101.
(11) Adelman, J.; Sachtler, W. M. H. *Appl. Catal., B* **1997**, *14*, 1.
(12) Descorme, C.; Gelin, P.; Primet, M.; Lecuyer, C. *Catal. Lett.* **1996**, *41*, 133.
(13) Aylor, A.; Lobree, L.; Reimer, J.; Bell, A. T. *J. Catal.* **1997**, *170*, 390.
(14) Sedlmair, C.; Gil, B.; Seshan, K.; Jentys, A.; Lercher, J. A. *Phys. Chem. Chem. Phys.* **2003**, *5*, 1897.
(15) Kuroda, Y.; Yagi, K.; Horiguchi, N.; Yoshikawa, Y.; Kumashiro, R.; Nagao, M. *Phys. Chem. Chem. Phys.* **2003**, *5*, 3318.
(16) Centi, G.; Gally, A.; Perathoner, S. *J. Chem. Soc., Faraday Trans.* **1996**, *92*, 5129.
(17) Valyon, J.; Keith Hall, W. In *Proceedings of the 10th International Congress on Catalysis*, Budapest, July 19−24, 1992; Elsevier: Amsterdam, The Netherlands, 1993; p 1339.
(18) Berlier, G.; Bonino, F.; Zecchina, A.; Bordiga, S.; Lamberti, C. *ChemPhysChem* **2003**, *4*, 1073.
(19) Ziolek, M.; Sobczak, I.; Nowak, I.; Decyk, P.; Stoch, J. *Stud. Surf. Sci. Catal.* **2001**, *135*, 1146.
(20) Battiston, A. A.; Bitter, J. H.; Koningsberger, D. C. *J. Catal.* **2003**, *218*, 163.
(21) Hadjiivanov, K.; Saussey, J.; Freysz, J.-L.; Lavalley, J.-C. *Catal. Lett.* **1998**, *52*, 103.
(22) Szanyi, J.; Paffett, M. T. *J. Catal.* **1996**, *164*, 232.
(23) Hoost, T. E.; Laframboise, K. A.; Otto, K. *Catal. Lett.* **1995**, *33*, 105.
(24) Szanyi, J.; Kwak, J. H.; Moline, R. A.; Peden, C. H. F. *Phys. Chem. Chem. Phys.* **2003**, *5*, 4045.

Table 1. IR Bands of Nitrogen Oxides[27]

species	mode	frequency (cm^{-1})
N$_2$O (gas)	ν(N–N)	2224
	ν(N–O)	1285
NO (gas)	ν(N–O)	1876
cis-(NO)$_2$	ν_s(N–O)	1870–1863
	ν_{as}(N–O)	1785–1760
trans-(NO)$_2$	ν_{as}(N–O)	1764
(ONON)	ν(–O=N)	1778
	ν(–N=O)	1690
N$_2$O$_3$ (gas)	ν_s(NO$_2$)	1652
	ν_{as}(NO$_2$)	1305
	ν(N–O)	1832
N$_2$O$_3$ (solid)	ν_s(NO$_2$)	1589
	ν_{as}(NO$_2$)	1297
	ν(N–O)	1863
NO$_2$ (gas)	ν_{as}(NO$_2$)	1612
N$_2$O$_4$ (gas)	ν_{as}(NO$_2$) (in phase)	1756–1730
	ν_{as}(NO$_2$) (out-of-phase)	1711 (shoulder)
	ν_s(NO$_2$)	1368–1359
N$_2$O$_5$ (covalent)	ν_s(NO$_2$)	1383
	ν_{as}(NO$_2$)	1728
N$_2$O$_5$ (ionized)	ν_{as}(NO$_2^+$)	2375
	ν_3(NO$_3^-$)	1413

observed at somewhat higher frequencies with other zeolites.[25,26]

(3) At a high oxygen concentration, reversibly adsorbed N$_2$O$_3$ (bands at 1875 and 1587 cm^{-1}) and N$_2$O$_4$ (1745 cm^{-1}) are formed.[22]

(4) A new species which has not been unambiguously assigned is also produced at high oxygen concentration. It absorbs at 2185 cm^{-1} and according to Szanyi and Paffett[22] is produced at the expense of the NO$^+$ band at 2133 cm^{-1}. Now, many authors assign this band tentatively to the [NO$^+$][NO$_2$] adducts.[6,24]

There are no works reporting low temperature NO adsorption and NO + O$_2$ coadsorption on H–ZSM-5 or other H-zeolites. In principle, low temperature NO adsorption is not widely investigated, since at low temperature NO forms dimers[27] and it is (NO)$_2$ that is the real adsorbate. However, it is possible to obtain important information on the surface properties of the adsorbents by studying NO adsorption at low temperature.[28,29]

In the pilot communication of this study,[30] we reported that NO$^+$ reacts with NO at low temperature, thus producing an [ONNO]$^+$ complex. The latter is characterized by ν_s(NO) at 2000 cm^{-1} and ν_{as}(NO) at 1687 cm^{-1}. In this work, we provide a more detailed study of NO adsorption and NO + O$_2$ coadsorption on H–ZSM-5 for different stoichiometries and temperatures and draw more definite conclusions about the nature and structure of the species formed. For a better assignment of the spectra, we have involved isotopic labeled compounds in some experiments.

2. Experimental Section

The H–ZSM-5 material was supplied by Degussa and had a Si/Al ratio of 26.8. The IR spectra were recorded on Nicolet Magna IR-550 and Nicolet Avatar 360 spectrometers at a spectral resolution of 2–4 cm^{-1} accumulating 64–128 scans. Self-supporting pellets were prepared from the sample powder and treated directly in purpose-made IR cells. The latter allowed measurement at room and low temperature and were connected to a conventional vacuum-adsorption apparatus. Prior to the adsorption measurements, the samples were activated by heating for 1 h in oxygen at 623 K and 1 h evacuation at the same temperature. Nitrogen monoxide was supplied by Air Liquide, France (99.9), and by Messer Griesheim GmbH (>99.0). ^{15}NO was purchased from ONIA and had an isotopic purity of 98.5 atom %. Before adsorption, oxygen was purified by passing it through a liquid nitrogen trap.

3. Results and Discussion

A large number of IR bands due to N$_x$O$_y$ species were observed in this study. For the sake of convenience, the spectral performance of different nitrogen oxides is recalled in Table 1, while the assignments of the bands observed in this study are summarized in Table 2.

3.1. Sample Characterization. The IR spectrum of the activated H–ZSM-5 sample contains, in the ν(O–H) region, a sharp band at 3610 cm^{-1} which characterizes the O–H stretching modes of the so-called acidic zeolite hydroxyls. In addition, a weak band at 3743 cm^{-1} is also visible and is assigned to silanol groups.

3.2. NO Adsorption at Ambient and Low Temperature. Adsorption of NO at room temperature on the H–ZSM-5 sample does not lead to formation of any adsorption species. Only two very weak bands at 1830 and 1637 cm^{-1} are discernible in the difference spectra and have been assigned to a negligible amount of adsorbed N$_2$O$_3$.

Introduction of NO (133 Pa) to the sample at 100 K leads to the appearance of one weak band at 1891 cm^{-1} (Figure 1, spectrum a). Simultaneously, the 3610 cm^{-1} OH band decreases in intensity and a new, broader band at 3373 cm^{-1} develops instead (see the left inset in Figure 1). These results allow us to assign the 1891 cm^{-1} band to NO which is H-bonded to the zeolite acidic OH groups. The observed ~240 cm^{-1} red shift of the O–H modes is consistent with the high acidity of these hydroxyls. For instance, the shift of this OH band provoked by adsorption of CO is ~300 cm^{-1},[31] which is due to the fact that CO is a stronger electrostatic base than NO.[32]

With time, the band at 1891 cm^{-1} rises in intensity (Figure 1, spectra b–d) and reaches saturation (Figure 1, spectra d and e). The shift of the 3610 cm^{-1} band follows the changes of the band at 1891 cm^{-1}. A series of new bands appears when the sample is in contact with NO at

**Table 2. Bands Due to N$_x$O$_y$ Species on H–ZSM-5**

species	formation conditions	^{14}N-bands (cm^{-1})	^{15}N-bands (cm^{-1})
OH–NO	NO adsorption at 100 K	1891	1860
OH(NO)$_2$	NO adsorption at 100 K	1872 and 1819	
cis-(NO)$_2$	NO adsorption at 100 K	1861 and 1762	
trans-(NO)$_2$	NO adsorption at 100 K	1784	1754
N$_2$O	interaction of NO with O$_2$ at T > 100 K	2227	
NO$^+$	NO + O$_2$ coadsorption at RT	2140–2133	2100
NO$^+$	NO + O$_2$ (excess) coadsorption at RT; oxidation of adsorbed (NO)$_2$ at 100 K	2206–2179	2150
[ONNO]$^+$	interaction of NO$^+$ and NO at 100 K	2000 and 1687	1965 and 1652
N$_2$O$_3$	oxidation of adsorbed NO	1904–1894, 1566, and 1303	1880, 1545, and 1297
N$_2$O$_3$	at T > 100 K	1864–1850, 1576, and 1325	1864
N$_2$O$_4$	coadsorption of NO and excess O$_2$	1742 and 1715 (w)	1702
NO$_2$	coadsorption of NO and excess O$_2$	1678–1643	1616
symmetric NO$_3^-$	coadsorption of NO and O$_2$	1380	
nitrites	coadsorption of NO and O$_2$	1447–1411	
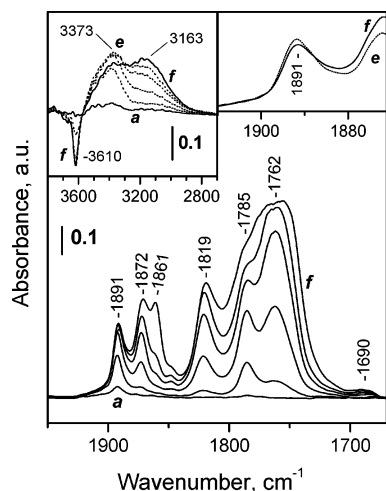
Figure 1. FTIR spectra of NO (133 Pa equilibrium pressure) adsorbed on H−ZSM-5 at 100 K. Spectrum taken immediately (a) and after 2 (b), 4 (c), 6 (d), 8 (e), and 10 min (f). The left inset shows the changes in the O−H stretching region. The right inset shows the changes in the N−O stretching region.


Figure 2. FTIR spectra of NO and O₂ coadsorbed on H−ZSM-5 at 100 K. Introduction of NO (133 Pa equilibrium pressure) followed by evacuation (a), after subsequent introduction of O₂ (133 Pa equilibrium pressure) (b), and evolution of the spectra during a gradual increase in the temperature in this atmosphere (c and d).

100 K, their maxima being at 1872, 1861, 1819, 1785, 1762, and 1690 (weak) cm^{-1} (Figure 1, spectra b–f). A band at 3163 cm^{-1} also develops in the O−H stretching region (Figure 1, spectra b–f). At high coverage, the bands at 1891 and 3373 cm^{-1} slightly decrease in intensity, while the intensity of the band at 3163 cm^{-1} increases (see the right inset in Figure 1). This indicates conversion of the OH−NO species into another compound. Evidently, these latter species are characterized by a band at 3163 cm^{-1}. The results strongly support the idea that, at high coverages, NO dimers H-bonded to the surface acidic hydroxyls are formed. These species are most likely characterized by bands at 1872 and 1819 cm^{-1}. Another type of (NO)₂ dimers is also formed and evidenced by bands at 1861 (ν_s) and 1762 cm^{-1} (ν_{as}). In addition, a strong band at 1785 cm^{-1}, attributed to *trans*-ONNO species, predominates at high coverages. A set of two weak bands at 2000 and 1690 cm^{-1} develops with time. These bands have been assigned to the [ONNO]$^+$ species.[30]

3.3. Interaction of Adsorbed NO with Oxygen. After adsorption of NO at 100 K, the sample was evacuated in order to remove the most labile adsorption forms. This procedure resulted in the disappearance of the set of bands at 1861 and 1762 cm^{-1} only (Figure 2, spectrum a). Then, oxygen (133 Pa initial pressure) was added into the cell. As a result, the spectrum changed drastically. All of the bands detected after NO adsorption disappeared (or strongly decreased in intensity), and a series of new bands emerged at 2207, 2180, 1904, 1762, 1742, 1715, 1566, 1411, 1380 (very weak), and 1303 cm^{-1} (Figure 2, spectrum b). The bands at 3366 and 3164 cm^{-1} in the O−H stretching region also vanished, and a new band at 3500 cm^{-1} (due to OH groups interacting with adsorbed species) was
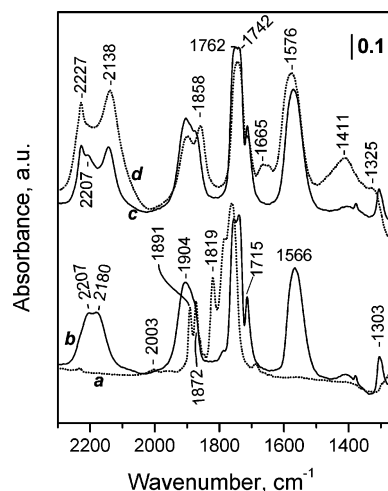
registered instead. The bands at 2207 and 2180 cm^{-1} are assigned to the N−O modes of two kinds of NO$^+$ species.[21] Alternatively, the higher frequency band could arise from NO₂$^+$.[23] The bands at ~1904, ~1566, and ~1303 cm^{-1} correspond to adsorbed N₂O₃. The two bands at 1742 and 1715 cm^{-1} are typical of N₂O₄.[32] Most likely, the band at 1762 cm^{-1} arises from some unreacted (NO)₂. Indeed, this band declines with time. The weak band at 1380 cm^{-1} probably characterizes symmetric nitrates. The band at 1411 cm^{-1} is assigned to nitrite species. Usually surface nitrates and nitrites are formed with the participation of Lewis acid sites, but they could also be produced as a result of disproportionation of nitrogen oxides, for example, according to the following reaction:

$$N_2O_4 \rightarrow [NO^+][NO_3^-] \qquad (4)$$
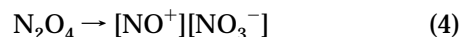
The results obtained imply that even at 100 K adsorbed NO is readily oxidized on the surface of the H−ZSM-5 sample. In the gas phase, this process is relatively slow, since the NO oxidation is a trimolecular reaction (see eq 1).

The temperature was then gradually increased in order to allow the "frozen" species to be converted into possibly more stable species or to migrate to more suitable adsorption sites. Initial heating led to the disappearance of the bands at 2207 and 2180 cm^{-1}, and two new bands developed at 2227 and 2138 cm^{-1} (Figure 2, spectra c and d). In addition to these changes, a broad band at 2490 cm^{-1} emerged, produced by the so-called B-feature of the acidic OH groups interacting with H₂O molecules. The corresponding less intense A-feature at ~2910 cm^{-1} was detected at further stages of the experiment. It is known[21] that formation of NO$^+$ in cationic positions is accompanied by water evolution (see eqs 1−3). Thus, the results indicate that NO$^+$ migrates when the temperature increases and starts to occupy cationic positions in the zeolite. In addition, two bands at 1665 and 1411 cm^{-1} develop. The N₂O₄ bands in the 1750−1700 cm^{-1} region initially slightly rise and then decline. A band at 1858 cm^{-1} develops but starts to decrease at higher temperatures. At the same time, the band at 1566 cm^{-1} is shifted to 1576 cm^{-1} and the band at 1303 cm^{-1}, to 1325 cm^{-1}. The band at 1380 cm^{-1} disappears.

(25) Gerlach, T.; Schütze, F.-W.; Baerns, M. *J. Catal.* **1999**, *185*, 131.
(26) Henriques, C.; Marie, O.; Thibault-Starzyk, F.; Lavalley, J.-C. *Microporous Mesoporous Mater.* **2001**, *50*, 167.
(27) Laane, J.; Ohlsen, J. R. *Prog. Inorg. Chem.* **1986**, *28*, 465.
(28) Bordiga, S.; Turnes Palomino, G.; Pazè, C.; Zecchina, A. *Microporous Mesoporous Mater.* **2000**, *34*, 67. Bordiga, S.; Lamberti, C.; Turnes Palomino, G.; Geobaldo, F.; Arduino, D.; Zecchina, A. *Microporous Mesoporous Mater.* **1999**, *30*, 129.
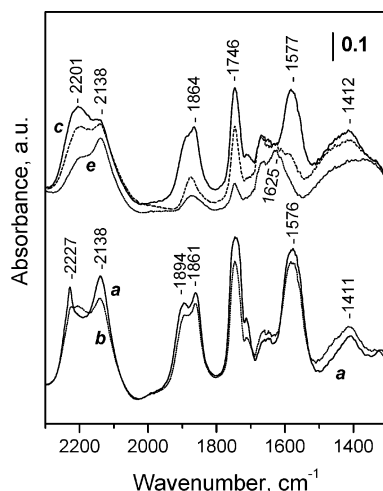(29) Hadjiivanov, K.; Concepción, P.; Knözinger, H. *Top. Catal.* **2000**, *11/12*, 123.
(30) Hadjiivanov, K.; Penkova, A.; Daturi, M.; Saussey, J.; Lavalley, J.-C. *Chem. Phys. Lett.* **2003**, *377*, 642.
(31) Hadjiivanov, K. I.; Vayssilov, G. N. *Adv. Catal.* **2002**, *47*, 307.
(32) Hadjiivanov, K. I. *Catal. Rev.−Sci. Eng.* **2000**, *42*, 71.

Figure 3. FTIR spectra of NO and O_2 coadsorbed on H−ZSM-5 (continuation of Figure 2). Evolution of the spectra during a gradual increase in the temperature up to ambient temperature (c−e).

Figure 4. FTIR spectra of NO and O_2 coadsorbed on H−ZSM-5. Introduction of NO (400 Pa equilibrium pressure) and O_2 (200 Pa equilibrium pressure) (a) and evolution of the spectra during subsequent gradual cooling (b−d).

The band at 2227 cm^{-1} is due to the N−N stretching modes of adsorbed N_2O.[32] The results indicate that N_2O is produced above 100 K from NO in the presence of oxygen. The band at 2138 cm^{-1} is assigned to NO$^+$ in cationic positions.[21] The band at 1665 cm^{-1} could be due to adsorbed NO_2, and that at 1411 cm^{-1}, to nitrite species. Alternatively, both bands could characterize symmetric O−N−O−N−O. This compound is formed during low temperature NO + O_2 co-condensation.[27] The results also suggest that during the temperature increase a second type of adsorbed asymmetric N_2O_3 species is formed. This compound is characterized by bands at ∼1858−1864, ∼1576, and ∼1325 cm^{-1}.

In summary, an increase in the temperature leads to rearrangement of some species, such as NO$^+$ (migrating to cationic positions) and N_2O_3, which reflects in some changes in their spectral performance.

Additional temperature increase is accompanied by a gradual decrease in intensity of the bands already assigned to different types of N_2O_3 and N_2O_4 species (Figure 3). Simultaneously, in the low frequency region, a band at 1625 cm^{-1} develops. This band arises from adsorbed water evolved during the production of NO$^+$ in cationic positions.

In the region around 2200 cm^{-1}, further heating provokes a decrease in intensity and the disappearance of the N_2O band at 2227 cm^{-1}. The NO$^+$ band at 2138 cm^{-1} progressively decreases in intensity, and a new band at 2201 cm^{-1} develops (Figure 3, spectra a−c) and then declines (Figure 3, spectra d and e). Evacuation at ambient temperature leads to the disappearance of both bands. However, the band at 2138 cm^{-1} is much more resistant.

3.4. Coadsorption of NO and O_2 at Room and Decreasing Temperature. A series of experiments were performed in order to estimate to what extent the temperature changes are reversible. In the first series of experiments, the amount of oxygen was close to the stoichiometric one (calculated for oxidation of NO to NO_2). NO (400 Pa) and O_2 (200 Pa) were coadsorbed on H−ZSM-5 at room temperature. As a result, a strong NO$^+$ band appeared in the IR spectrum at 2133 cm^{-1} (Figure 4, spectrum a). In addition, weak bands at 1900 and 1555 cm^{-1} (N_2O_3) and 1620 cm^{-1} (H_2O) were also visible (Figure 4, spectrum a). Cooling the sample in this atmosphere leads to the following changes (Figure 4, spectra b−d):

(1) There is a slight increase in intensity of the N_2O_3 bands which are settled at 1915 and 1557 cm^{-1}.
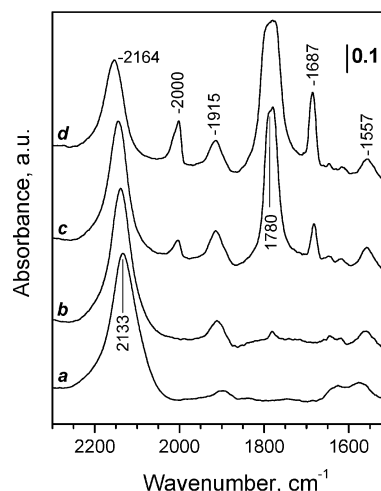
(2) A strong band develops at ∼1780 cm^{-1}. This band is assigned to the adsorbed (NONO) dimer.[27]

(3) There is a gradual decrease in intensity of the band at 2133 cm^{-1} and a gradual blue shift of its maximum to 2164 cm^{-1}. Simultaneously, a set of two new bands at 2000 and 1687 cm^{-1}, attributed to the positively charged [ONNO]$^+$ dimer,[30] developed. The band at 2000 cm^{-1} was assigned to the symmetric N−O stretching modes, and that at 1687 cm^{-1}, to the corresponding antisymmetric modes.

Subsequent heating leads to back conversion of the bands at 2164 and 2000 cm^{-1} into the band at ∼2138 cm^{-1}; that is, the [ONNO]$^+$ species is decomposed to NO$^+$ and NO.

The observed changes were found to be generally the same after further cooling−heating cycles. However, the behavior of the N_2O_3 bands is interesting. Cooling leads to the appearance of the adsorption form characterized by a band at 1915−1910 cm^{-1}, while the band at ∼1850 cm^{-1} is produced during the heating cycles. This suggests a phase transition typical of already adsorbed N_2O_3.

Another set of experiments was performed on coadsorption of NO with increasing amounts of oxygen. Initially, NO (500 Pa) and O_2 (133 Pa) were coadsorbed on the sample. A strong NO$^+$ band at 2133 cm^{-1} and two N_2O_3 bands at 1900 and 1572 cm^{-1} were registered (Figure 5, spectrum a). Then, the amount of oxygen was gradually increased up to an initial partial pressure of 1 kPa. This led initially to growing (formation) and then to a decline (oxidation) of the N_2O_3 bands (Figure 5, spectra b−d). Bands due to adsorbed N_2O_4 (1745 cm^{-1}) and NO_2 (1678 cm^{-1}) continuously increased. A broad band at ∼1440 cm^{-1} also appeared. In the region around 2200 cm^{-1}, the NO$^+$ band at 2133 cm^{-1} gradually decreased in intensity and a new band at 2205 cm^{-1} developed instead.

Cooling of the sample results in a fast decrease in intensity of the N_2O_4 band at 1745 cm^{-1} (Figure 6). Since no other bands have been developed at its expense, we believe that this phenomenon is due to migration of the N_2O_4 from the sample to the colder parts in the IR cell. This is normal for weak adsorption forms. In addition, a band at ∼1900 cm^{-1} also develops and then declines. This band is attributed to adsorbed N_2O_3 which, similar to N_2O_4, migrates to the coldest parts of the system. The intensity of the band at 1425 cm^{-1} is enhanced. The NO$^+$ band at 2141 cm^{-1} disappears and is gradually converted into a
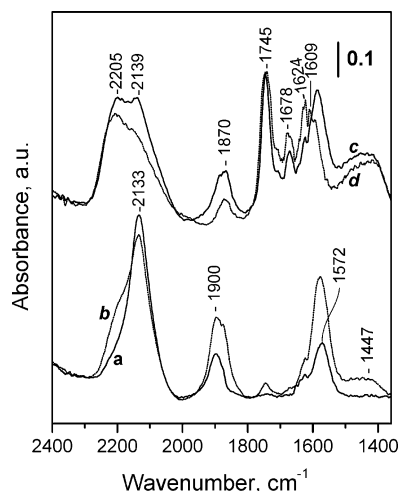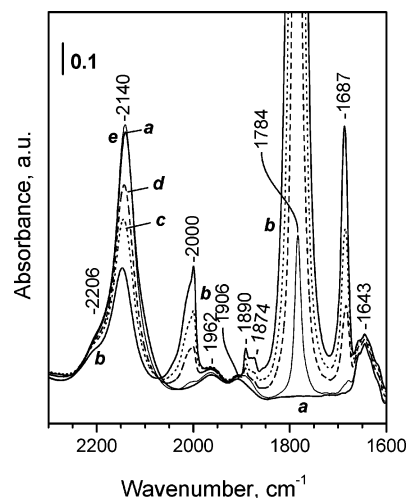
Figure 5. FTIR spectra of NO and O$_2$ coadsorbed on H−ZSM-5 at 293 K. Introduction of NO (500 Pa equilibrium pressure) and O$_2$ (133 Pa equilibrium pressure) (a) and after increasing the formal partial oxygen pressure to 300 (b), 600 (c), and 1000 Pa (d).
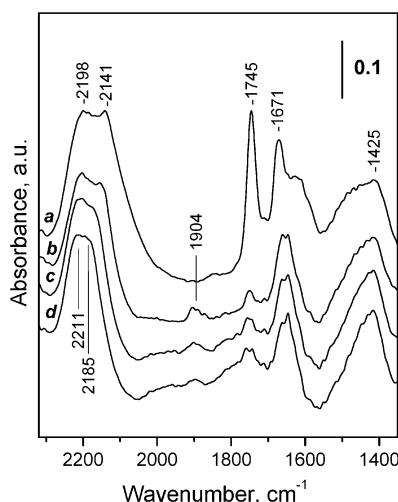
Figure 6. FTIR spectra of NO and O$_2$ coadsorbed on H−ZSM-5 (continuation of Figure 2). Coadsorption of NO (500 Pa equilibrium pressure) and O$_2$ (1000 Pa equilibrium pressure) (a) and evolution of the spectra during gradual cooling of the sample (b−d).

broad band with two resolved maxima at 2211 and 2185 cm^{-1}. An important conclusion of these results is that the bands above 2200 cm^{-1} do not arise from [NO$^+$][NO$_2$] or [NO$^+$][N$_2$O$_4$] adducts.

3.5. Interaction of Adsorbed Species with NO. To obtain more information on the nature of the [ONNO]$^+$ species, we performed some additional experiments. Initially, NO (665 Pa) and O$_2$ (133 Pa) were coadsorbed at room temperature. Then, the sample was cooled to 100 K. As a result, a strong NO$^+$ band at 2140 cm^{-1}, N$_2$O$_3$ bands at 1962, 1906, 1589, and 1558 cm^{-1}, and a NO$_2$ band at 1643 cm^{-1} were detected (Figure 7, spectrum a). Then, NO was introduced into the cell. A very strong band at 1784 cm^{-1} (*trans*-NO dimer) developed, and two weak bands at 1890 and 1874 cm^{-1} also emerged (Figure 7, spectrum b). The latter were observed after NO adsorption on H−ZSM-5 and were already assigned to H-bonded NO and NO dimers, respectively. The intensity of these bands is strongly reduced in this case, since an important fraction of the acidic hydroxyls have reacted to give water and NO$^+$ in cationic positions.

Figure 7. FTIR spectra of NO and O$_2$ coadsorbed on H−ZSM-5. Introduction of NO (665 Pa) and O$_2$ (133 Pa) at ambient temperature and cooling to 100 K (a), after subsequent introduction of NO (665 Pa) (b), and development of the spectra under dynamic vacuum (c−e).

In addition, the NO$^+$ band at 2140 cm^{-1} strongly decreases in intensity and bands due to [ONNO]$^+$ at 2000 and 1687 cm^{-1} appear instead. This indicates that the following reaction has proceeded:

$$NO^+ + NO \rightarrow [ONNO]^+ \qquad (5)$$

A careful inspection of the spectra shows that, in addition to the band at 2140 cm^{-1}, its high frequency shoulder at 2206 cm^{-1} also decreases in intensity after introduction of NO. This observation strongly supports the idea that the band at 2206 cm^{-1} also characterizes NO$^+$ species.

Subsequent evacuation (Figure 7, spectra c−e) leads to gradual development of the initial spectrum: the bands at 1890, 1874, and 1784 cm^{-1} quickly disappear; the bands at 2000 and 1687 cm^{-1} decrease in concert; and the band at 2140 cm^{-1} together with its satellite at 2206 cm^{-1} develops at their expense; that is, the reverse of eq 5 occurs.

3.6. Experiments Involving ^{15}NO. To support the assignment of the different bands, experiments involving ^{15}NO were performed. The positions of the observed bands are summarized in Table 2. Here, only the most important and key results will be discussed.

After coadsorption of ^{15}NO and O$_2$, a ^{15}NO$^+$ band at 2100 cm^{-1} with a shoulder at 2150 cm^{-1} develops. In addition, bands due to adsorbed ^{15}N$_2$O$_3$ (1853 and 1548 cm^{-1}), ^{15}N$_2$O$_4$ (1704 cm^{-1}), and ^{15}NO$_2$ (1602 cm^{-1}) are also observed. The experimental isotopic shifts coincide very well with the theoretically calculated one. A decrease in the total equilibrium pressure leads to a fast decline of the ^{15}N$_2$O$_3$ bands followed by the ^{15}N$_2$O$_4$ bands, the ^{15}NO bands, and the high frequency shoulder of the ^{15}NO$^+$ band.

The sample was cooled to 100 K and shortly evacuated. After this treatment, the ^{15}NO$^+$ band was registered at 2104 cm^{-1}, the bands of ^{15}N$_2$O$_3$, at 1885 and 1552 cm^{-1}, the band of *trans*-(^{15}NO)$_2$, at 1753 cm^{-1}, and the band of ^{15}NO$_2$, at 1616 cm^{-1}. Subsequent introduction of ^{15}NO (500 Pa) provokes a strong increase in intensity of the band at 1754 cm^{-1}. The ^{15}NO$^+$ band and its satellite (observed at 2140 and 2095 cm^{-1}, respectively, in the difference spectra) decrease in intensity, and two new bands, at 1965 and 1652 cm^{-1}, develop (Figure 8, spectra a and b). These two bands are assigned to the [O^{15}N^{15}NO]$^+$ species. The band at 1965 cm^{-1} has a pronounced high frequency shoulder at 1977 cm^{-1}. This suggests that the NO$^+$ species
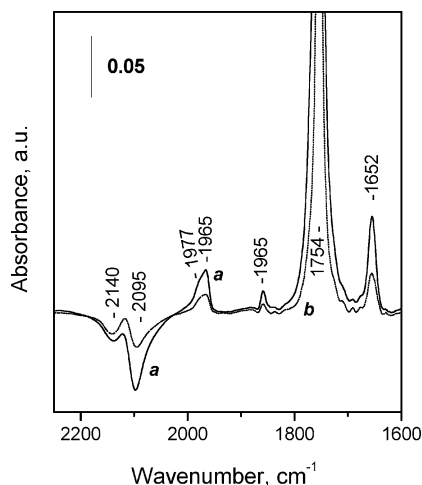
Figure 8. Difference FTIR spectra of ^{15}NO and O_2 coadsorbed on H−ZSM-5. Initially ^{15}NO (665 Pa) and O_2 (∼65 Pa) were introduced to the sample at ambient temperature, and then the system was cooled to 100 K (background spectrum). Spectrum a presents the changes registered after subsequent introduction of ^{15}NO (133 Pa) to the system, and spectrum b is obtained after a short evacuation.
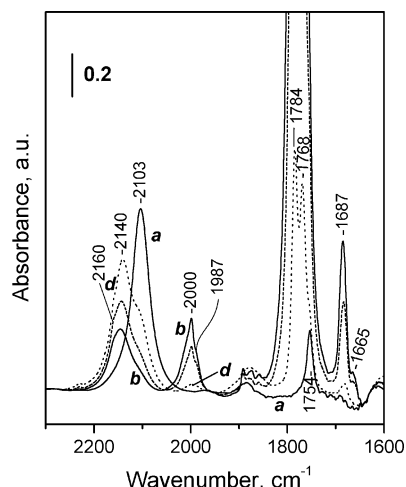
Figure 9. FTIR spectra of ^{15}NO and O_2 coadsorbed on H−ZSM-5. Introduction of ^{15}NO (665 Pa) and O_2 (∼65 Pa) at ambient temperature and cooling to 100 K (a), after subsequent introduction of ^{14}NO (665 Pa) to the system (b), and development of the spectra under dynamic vacuum (c and d).

characterized by a band at 2140 cm^{-1} form positively charged dimers observable at 1976 cm^{-1}, while the 2097 cm^{-1} NO$^+$ species produce dimers monitored at 1965 cm^{-1}. Evidently, the antisymmetric mode at ∼1652 cm^{-1} is not sensitive to the environment.

Some experiments aiming at isolation of dimer species having one ^{14}N atom and one ^{15}N atom were also carried out. Initially, coadsorption of ^{15}NO and O_2 was performed and then the system was cooled. A strong $^{15}NO^+$ band was detected at 2103 cm^{-1}. Weak bands due to *trans*-($^{15}NO)_2$ and $^{15}N_2O_3$ were registered at 1754 and 1883 cm^{-1}, respectively. (Figure 9, spectrum a). Then, ^{14}NO (665 Pa) was added to the system. As a result, the $^{15}NO^+$ band strongly decreased in intensity and was shifted to higher frequencies (typical of those of $^{14}NO^+$), indicating a fast isotopic exchange (Figure 9, spectrum b). A strong band at 1784 cm^{-1} with a shoulder at 1768 cm^{-1} appeared. Two intense [ONNO]$^+$ bands at 2000 and 1687 cm^{-1} were also detected. Careful analysis of the spectra showed that the band at 2000 cm^{-1} had a lower frequency shoulder at 1987 cm^{-1}, while the band at 1687 cm^{-1} demonstrated a
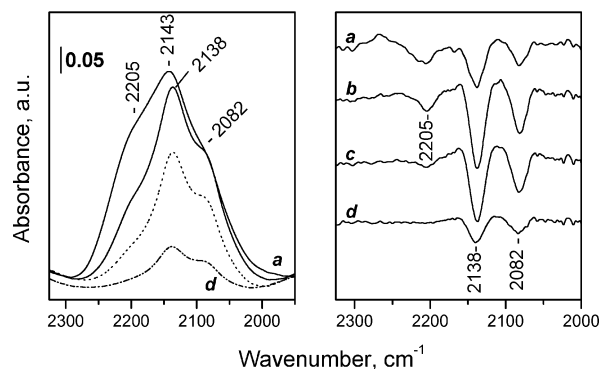
Figure 10. Left panel: FTIR spectra of NO and $^{18}O_2$ coadsorbed on H−ZSM-5. Introduction of NO (200 Pa) and O_2 (400 Pa) at ambient temperature (a), after a decrease in the total pressure to 200 (b) and ∼100 Pa (c), and after a short evacuation (d). Right panel: Second derivative of the spectra presented in the left panel.

shoulder at 1665 cm^{-1}. Under the conditions of the experiments, there was an excess of ^{14}N in the nitrogen-oxo compounds, which indicates that the majority of the species had two ^{14}N atoms and some of them had one ^{14}N atom and one ^{15}N atom. Hence, the bands at 1987 and 1665 cm^{-1} originated from the [($^{14}NO)(^{15}NO)]^+$ species. Note that a similar situation was observed with the ν_{as} modes of the trans-dimer of NO (see Figure 9, spectrum b). The results allow us to assign the bands at 2000 and 1687 cm^{-1} to the ν_s and ν_{as} modes, respectively, of the [O$^{14}N^{14}NO]^+$ species. Since both modes are IR active, the complex has a cis-configuration. Evidently, the positive charge in these complexes is delocalized. These species are easily decomposed during evacuation to NO$^+$ and NO (Figure 9, spectra c and d), which is consistent with the fast isotopic exchange observed in this study.

3.7. Experiments Involving $^{18}O_2$. To support additionally the proposed assignments, we have also performed some experiments involving $^{18}O_2$. They mainly concern the correct assignment of the bands at ∼2200 cm^{-1} to NO$^+$ or NO$_2^+$. NO (200 Pa initial equilibrium pressure) and $^{18}O_2$ (400 Pa initial equilibrium pressure) were coadsorbed on H−ZSM-5, and the spectrum was recorded after 1 h. A complex band appeared in the 2300−2000 cm^{-1} region (Figure 10, left panel, spectrum a). It had a distinguished maximum at 2143 cm^{-1} and two shoulders at lower and at higher frequencies. To establish the exact positions of the maxima, we used the second derivative of the spectra (see the right panel of Figure 10). The results indicate the existence of three bands with maxima at 2205, 2138, and 2082 cm^{-1}. A decrease in the total equilibrium pressure and evacuation lead to a decline of the band at 2205 cm^{-1} (Figure 10, spectra b−d). The other bands also decrease in intensity.

The band at 2138 cm^{-1} is unambiguously assigned to the N−O stretching modes of the N$^{16}O^+$ species. Using the isotopic shift factor, the corresponding N−^{18}O mode is expected at 2082 cm^{-1}. This allows assignment of the band at 2082 cm^{-1} to the N$^{18}O^+$ species.

The band at 2205 cm^{-1} could correspond to the NO$^+$ or NO$_2^+$ species. In both cases, the corresponding N−O modes after a full $^{16}O \rightarrow ^{18}O$ exchange are expected at 2147 cm^{-1}. Evidently, in our spectra, this band is masked by the strong band at 2138 cm^{-1}. Only when the concentration of the species is relatively high (Figure 10, right panel, spectrum a), the band could be seen as a shoulder. Analysis of the intensities of the different bands indicates that the ratio between the ^{16}O- and ^{18}O-containing nitrogen-oxo species is ∼3:2. Under these conditions, if the species were NO$_2^+$,

a significant part of them should have contained one ^{16}O atom and one ^{18}O atom. This should have led to the appearance of a strong band around 2176 cm^{-1}. Since no such band was detected, we infer that the 2205 cm^{-1} band characterizes the NO^{+} species. This conclusion is consistent with the above observations that the species under consideration are converted, in the presence of NO, into the [ONNO]$^{+}$ species.

Some authors[6,24] have tentatively assigned the 2205 cm^{-1} band to the [NO^{+}][NO$_2$] adducts. Our results indicate that the 2205 cm^{-1} band arises from the NO^{+} species occupying different positions from those of the species observed with a band at 2133 cm^{-1}. Formation of some adsorbed species most probably induces migration of the NO^{+} species from the cationic positions. However, no [NO^{+}]-[NO$_2$] complexes are formed.

3.8. Changes in the O−H Stretching Region. To check for possible participation of OH groups in the formation of different species, we have examined the spectra in the O−H stretching region. Introduction of a NO + O$_2$ mixture and cooling to 100 K results in a strong decrease in intensity of the 3610 cm^{-1} band because of the formation of NO^{+} occupying cationic positions (Figure 11, spectrum a). Subsequent NO introduction leads to a small additional decrease in intensity of the band at 3610 cm^{-1} and development of a broad band at 3380 cm^{-1} (Figure 11, spectrum b). These changes have been registered after NO adsorption only and attributed to formation of H-bonded NO. In addition, two bands at 3764 and 3470 cm^{-1} develop and disappear after subsequent evacuation. The same bands are found at lower frequencies (3698 and 3405 cm^{-1}, respectively) when ^{15}NO is used for the experiments. These results prove that the bands are not related to O−H stretching modes but are due to overtones/combination modes of N−O stretches. In particular, we assign the band at 3764 cm^{-1} to the ($\nu_\text{s} + \nu_\text{as}$) mode and that at 3470 cm^{-1} to the (2ν_as) mode of the *trans*-(NO)$_2$ dimer. Thus, the results obtained prove that no OH groups are involved in the formation of [ONNO]$^{+}$ from NO^{+} and NO.

4. Conclusions

(1) Low temperature NO adsorption on H−ZSM-5 leads to the formation of (i) NO H-bonded to the acidic hydroxyls,
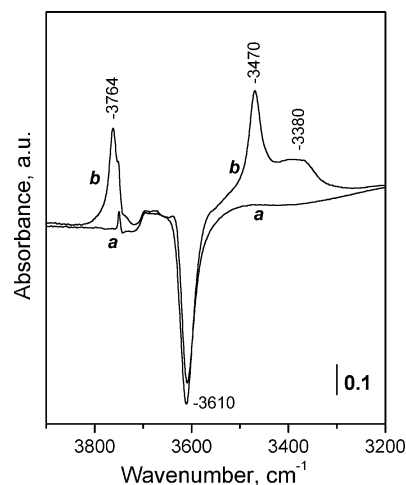
Figure 11. Difference FTIR spectra in the O−H stretching region. Changes of the spectra after introduction of NO (665 Pa) and O$_2$ (133 Pa) at ambient temperature to H−ZSM-5 and cooling to 100 K (a) and after subsequent introduction of NO (665 Pa) (b).

which are converted, at higher coverage, into H-bonded dimers; (ii) *cis*-(NO)$_2$; and (iii) *trans*-(NO)$_2$.

(2) The NO adsorption species are oxidized fast by oxygen at 100 K. N$_2$O$_3$, NO^{+}, NO$_2$, and N$_2$O$_4$ are among the reaction products. Different kinds of N$_2$O$_3$ species are detected.

(3) NO^{+} in a cationic position absorbs at 2133 cm^{-1} and adsorbs above this frequency when moved into another position.

(4) At low temperature, NO^{+} reacts with NO to give positively charged NO dimers, that is, [ONNO]$^{+}$. The latter species are characterized by ν_s at 2000 cm^{-1} and ν_as at 1967 cm^{-1}.